C-Nap1, a Novel Centrosomal Coiled-Coil Protein and Candidate Substrate of the Cell Cycle–regulated Protein Kinase Nek2

Andrew M. Fry,* Thibault Mayor,* Patrick Meraldi,* York-Dieter Stierhof,‡ Kayoko Tanaka,* and Erich A. Nigg*

*Department of Molecular Biology, Sciences II, University of Geneva, CH-1211 Geneva 4, Switzerland; and ‡Max-Planck-Institut für Biologie, Abteilung Membranbiochemie, D-72076 Tübingen, Germany

Abstract. Nek2 (for NIMA-related kinase 2) is a mammalian cell cycle–regulated kinase structurally related to the mitotic regulator NIMA of *Aspergillus nidulans*. In human cells, Nek2 associates with centrosomes, and overexpression of active Nek2 has drastic consequences for centrosome structure. Here, we describe the molecular characterization of a novel human centrosomal protein, C-Nap1 (for centrosomal Nek2-associated protein 1), first identified as a Nek2-interacting protein in a yeast two-hybrid screen. Antibodies raised against recombinant C-Nap1 produced strong labeling of centrosomes by immunofluorescence, and immunoelectron microscopy revealed that C-Nap1 is associated specifically with the proximal ends of both mother and daughter centrioles. On Western blots, anti–C-Nap1 antibodies recognized a large protein (>250 kD) that was highly enriched in centrosome preparations. Sequencing of overlapping cDNAs showed that C-Nap1 has a calculated molecular mass of 281 kD and comprises extended domains of predicted coiled-coil structure. Whereas C-Nap1 was concentrated at centrosomes in all interphase cells, immunoreactivity at mitotic spindle poles was strongly diminished. Finally, the COOH-terminal domain of C-Nap1 could readily be phosphorylated by Nek2 in vitro, as well as after coexpression of the two proteins in vivo. Based on these findings, we propose a model implicating both Nek2 and C-Nap1 in the regulation of centriole–centriole cohesion during the cell cycle.

T HE serine/threonine kinase NIMA of *Aspergillus nidulans* is considered the founding member of a family of protein kinases with a possible role in cell cycle regulation (for reviews see Fry and Nigg, 1995; Lu and Hunter, 1995*a*; Osmani and Ye, 1996). In *A. nidulans*, NIMA clearly cooperates with the Cdc2 protein kinase to promote progression into mitosis (Osmani et al., 1991), and overexpression of NIMA in a variety of heterologous species promotes a premature onset of chromosome condensation (O'Connell et al., 1994; Lu and Hunter, 1995*b*). This has been interpreted to suggest evolutionary conservation of a pathway involving NIMA-related kinases (for review see Lu and Hunter, 1995*a*). Indeed, kinases structurally related to NIMA are present in many species (Fry and Nigg, 1997). However, the only bona fide functional homologue of NIMA so far isolated stems from another filamentous fungus, *Neurospora crassa* (Pu et al., 1995), and the functional relationship between vertebrate NIMA-related kinases and fungal NIMA remains uncertain.

The closest known mammalian relative to NIMA is a kinase termed Nek2 (for NIMA-related kinase 2)[1] (Fry and Nigg, 1997). This kinase undergoes cell cycle–dependent changes in abundance and activity, reminiscent of NIMA (Schultz et al., 1994; Fry et al., 1995). It is highly expressed in male germ cells (Rhee and Wolgemuth, 1997; Tanaka et al., 1997), and data have been reported consistent with a role for Nek2 in meiotic chromosome condensation (Rhee and Wolgemuth, 1997). However, overexpression of active Nek2 in somatic cells has no obvious effect on chromosome condensation; instead, it induces striking alterations in the structure of the centrosome, the principal microtubule-organizing center of mammalian cells (Fry et al., 1998). Furthermore, immunofluorescence microscopy and subcellular fractionation concur to demonstrate that endogenous Nek2 associates with centrosomes, strongly suggesting that one physiological function of this kinase may relate to the centrosome cycle (Fry et al., 1998).

Address all correspondence to Erich A. Nigg, Department of Molecular Biology, Sciences II, University of Geneva, 30, Quai Ernest-Ansermet, CH-1211 Geneva 4, Switzerland. Tel.: +41 22 702 6127. Fax: +41 22 702 6868. E-mail: erich.nigg@molbio.unige.ch

1. *Abbreviations used in this paper*: CDK, cyclin-dependent kinase; C-Nap1, centrosomal Nek2-associated protein 1; IEM, immunoelectron microscopy; INMP, intranuclear matrix protein; Nek2, NIMA-related kinase 2; PCM, pericentriolar material; SPB, spindle pole body; γ-TuRCs, γ-tubulin–containing ring complexes.

The mammalian centrosome is an organelle of about 1 μm in diameter. It comprises two barrel-shaped centrioles that are made of nine short triplet microtubules and are surrounded by an amorphous matrix known as the pericentriolar material (PCM) (for review see Brinkley, 1985; Vorobjev and Nadehzdina, 1987; Kimble and Kuriyama, 1992; Kalt and Schliwa, 1993; Kellogg et al., 1994; Lange and Gull, 1996). Major progress has recently been made with the demonstration that microtubules are nucleated from γ-tubulin–containing ring complexes (γ-TuRCs), which are concentrated within the PCM (Moritz et al., 1995; Zheng et al., 1995). γ-Tubulin forms complexes with Spc97/98, two evolutionarily conserved proteins first identified in budding yeast spindle pole bodies (Geissler et al., 1996; Knop et al., 1997; Stearns and Winey, 1997), and there is also evidence for an important role of pericentrin and other coiled-coil proteins in organizing γ-TuRCs into higher order lattice structures (Doxsey et al., 1994; Dictenberg et al., 1998). However, in spite of this recent progress, it is clear that the inventory of centrosome components is far from complete.

Centrosome structure and function is regulated in a cell cycle–dependent manner (for reviews see Mazia, 1987; Kellogg et al., 1994; Tournier and Bornens, 1994). Once in every cell cycle, and beginning around the G1/S transition, centrioles are duplicated (e.g., Kuriyama and Borisy, 1981*a*; Vorobjev and Chentsov, 1982; Kochanski and Borisy, 1990; Chrétien et al., 1997). Late in G2, centrosomes then grow in size (a process referred to as maturation) through the recruitment of additional PCM proteins (Rieder and Borisy, 1982; Kalt and Schliwa, 1993; Lange and Gull, 1995). At the G2/M transition, the duplicated centrosomes separate and migrate to opposite ends of the nucleus. Concomitantly, their microtubule-nucleating activities increase dramatically in preparation for spindle formation (McGill and Brinkley, 1975; Snyder and McIntosh, 1975; Gould and Borisy, 1977; Kuriyama and Borisy, 1981*b*; for reviews see Brinkley, 1985; Vorobjev and Nadehzdina, 1987; Karsenti, 1991). By what mechanisms these events are controlled remains largely unknown, but data obtained using phosphoepitope-specific antibodies strongly suggest that phosphorylation of centrosomal proteins plays a major role (Vandré et al., 1984, 1986; Centonze and Borisy, 1990). More direct support for this view stems from the observation that cyclin-dependent kinases (CDKs) enhance the microtubule-nucleation activity of centrosomes at the G2/M transition (Verde et al., 1990, 1992; Buendia et al., 1992) and are involved in promoting centrosome separation (Blangy et al., 1995; Sawin and Mitchison, 1995). Similarly, polo-like kinase 1, a cell cycle regulatory kinase structurally distinct from CDKs, has recently been implicated in centrosome maturation (Lane and Nigg, 1996).

The precise role of Nek2 at the centrosome remains to be determined, but it is intriguing that overexpression of this kinase in human cells causes a pronounced splitting of centrosomes. This led us to propose that Nek2-dependent phosphorylation of previously unidentified proteins may cause a loss of centriole–centriole cohesion, and that this event might represent an early step in centrosome separation at the G2/M transition (Fry et al., 1998). With the aim of identifying potential substrates (or regulators) of Nek2,

we have now performed a yeast two-hybrid screen, using full-length Nek2 as a bait. We report here the molecular characterization of a novel coiled-coil protein that we call C-Nap1 (for centrosomal Nek2-associated protein 1). C-Nap1 represents a core component of the mammalian centrosome and the first candidate substrate for a member of the NIMA protein kinase family to be identified.

Materials and Methods

Two Hybrid Interaction Screening

A yeast two-hybrid screen was performed essentially as described previously (Durfee et al., 1993; Harper et al., 1993; Blangy et al., 1997). In brief, yeast strain Y190 expressing the fusion protein GAL4 DBD-Nek2 was transformed with a human B cell cDNA library constructed in plasmid pACT (Durfee et al., 1993) and plated on selective medium (lacking tryptophan, leucine, and histidine) supplemented with 50 mM 3-aminotriazole. From 4×10^6 transformants, 43 His$^+$ colonies were obtained, of which 18 were positive for lacZ expression. Bait loss through cycloheximide selection was only successful for 11 out of 18. Of these, eight remained lacZ positive when mated with Y187 carrying DBD-Nek2, but were negative when mated with Y187 carrying DBD-p53, -lamin, -cdk2, -SNF1, or -Eg5. The library cDNAs in these eight positives were amplified by PCR, using pACT2-specific primers (AATACCACTACAATGGATGATG and GCTCTAGAGTTGAAGTGAACTTGCGGGG), and the PCR products were digested with the frequently cutting restriction endonuclease, AluI, to determine the number of different clones. Three clones (2-6, 2-27, and 2-31) contained an identical 1.7-kb insert, while a fourth clone (2-2) was slightly larger (1.9 kb) and yielded a very similar digestion pattern. For subsequent analyses, the PCR products from clones 2-6 and 2-2 were digested with EcoRI and XbaI and subcloned into the EcoRI-XbaI sites of a pBlueScript-KS vector carrying the myc-epitope tag (Schmidt-Zachmann and Nigg, 1993) to generate the plasmids pBSmyc:2-6 and pBSmyc:2-2. To construct the eukaryotic expression plasmid pCMVmyc:2-6, the myc:2-6 fusion was excised from pBSmyc:2-6 on a HindIII-XbaI fragment and subcloned into the HindIII-XbaI sites of pRcCMV (Invitrogen Corp., Carlsbad, CA).

Antibody Production

To generate antibodies, a (His)$_6$-tagged fusion protein of clone 2-6 was made using the QIAexpress bacterial expression system (QIAGEN, Inc., Valencia, CA). The plasmid pQE10:2-6 was constructed by subcloning a BamH1-XbaI (blunted with Klenow) fragment from pBSmyc:2-6 into the pQE10 vector (QIAGEN) digested with BamHI and HindIII (blunted with Klenow). Overexpression was found to be optimal in the *Escherichia coli* strain M15[pREP4] using Super medium (25 g bacto-tryptone, 15 g bacto-yeast extract, and 5 g NaCl per liter). Recombinant protein was expressed and purified under denaturing conditions as described by the manufacturer (QIAGEN), before concentrating on a Centricon-30 column (Amicon, Inc., Beverly, MA) and further purification on a preparative 12% SDS–polyacrylamide gel as described in Fry et al. (1998). For immunizations, 500 μg of the purified (His)$_6$:2-6 protein was injected subcutaneously into New Zealand white rabbits (Elevage Scientifique des Dombes, Chatillon sur Chalaronne, France) on days 1, 28, 56, and 84. Immune serum was obtained on days 70 and 98. For affinity purification of antibodies, two different methods were used. In the first, (His)$_6$:2-6 protein was expressed in *E. coli*, purified under native conditions and bound to a Ni^{2+}-resin column as described in the QIAexpress protocol handbook. Crude serum was applied to the column, and after washing, the antibody was eluted in 4 M MgCl$_2$ as described by Gu et al. (1994). The purified antibody was dialyzed extensively against PBS before use. In the second approach, 1.0 mg of purified (His)$_6$:2-6 protein was covalently coupled to 400 mg CNBr-activated Sepharose 4B (Pharmacia Biotech, Piscataway, NJ) as recommended by the manufacturer, and this affinity matrix was used to purify antibodies from immune serum as described by Harlow and Lane (1988).

Cell Culture and Transfections

Human U2OS osteosarcoma and KE37 T-lymphoblastoid cells were grown at 37°C in a 7% CO$_2$ atmosphere in DME supplemented with 10% heat-inactivated FCS and penicillin-streptomycin (100 IU/ml and 100 mg/ml,

respectively). Sf9 insect cells were grown in TC100 medium (GIBCO BRL, Gaithersburg, MD), supplemented with 10% heat-inactivated FCS and penicillin-streptomycin at 27°C. For transient transfection studies, U2OS cells were seeded onto HCl-treated glass coverslips at a density of 1×10^5 cells per 35-mm dish and transfected with 10 μg of plasmid DNA, using calcium phosphate precipitates as previously described (Krek and Nigg, 1991).

Immunofluorescence and Immunoelectron Microscopy

Immunofluorescence microscopy on U2OS cells was performed as described in Fry et al. (1998), using a Zeiss Axioplan II microscope (Thornwood, NY) and 40 or 63× oil immersion objectives. Affinity-purified anti–C-Nap1 antibodies (R62 and R63) were used at 1.0 μg/ml. Photographs were taken using a Quantix 1400 CCD camera (Photometrics, Inc., Tuscon, AZ) and IP-Lab software, and the images were processed using Adobe Photoshop (San Jose, CA).

Negative staining immunoelectron microscopy of isolated centrosomes was performed by diluting centrosomes 1:10 in PBS before sedimentation onto Pioloform and carbon-coated grids using an airfuge (65,000 g-av, 15 min; Beckman Instruments, Inc., Fullerton, CA). Grids were blocked with 0.1% gelatin in PBS, incubated with affinity-purified anti–C-Nap1 IgGs (R63, 1 μg/ml in blocking buffer, 45 min) and protein A–6-nm gold (60 min; Slot and Geuze, 1985). Grids were negatively stained with Nano-W (Nanoprobes, Stony Brook, NY). For preembedding immunoelectron microscopy of whole cells, U2OS cells, grown on coverslips, were fixed with 3% paraformaldehyde/2% sucrose for 10 min, permeabilized with PBS + 0.5% Triton X-100 for 5 min, and blocked with PBS + 1% BSA for 5 min. Cells were then labeled with either anti–C-Nap1 IgGs (R63, 1 μg/ml) or anti-Nek2 IgGs (R40, 1 μg/ml) followed by goat anti–rabbit IgG-Nanogold (1:40; Nanoprobes). Cells were further fixed with 2.5% glutaraldehyde in PBS for 60 min, washed with distilled water, and silver enhanced for 26 min using silver lactate/gum arabicum (Stierhof et al., 1991). After thoroughly washing with distilled water, cells were postfixed with 1% aqueous uranyl acetate, dehydrated in ethanol, and embedded in epoxy resin (EPON®; Shell Chemical Co.). After polymerization, the EPON® layer containing the cells was separated from the coverslip by dipping into liquid nitrogen. Ultrathin sections were cut in parallel to the monolayer and stained with aqueous uranyl acetate and lead citrate.

Cell Extracts, Immunoblotting, and Phosphorylation Assays

To prepare cell extracts for immunoblotting, cells were harvested and washed once in PBS + 1 mM PMSF before resuspending in extraction buffer (50 mM Tris-HCl, pH 7.5, 1% Triton X-100, 150 mM NaCl, 5 mM EDTA, 1 mM PMSF, 1 μg/ml aprotinin, 1 μg/ml leupeptin, 1 μg/ml pepstatin A, 20 mM β-glycerophosphate) to give 10^4 cells/μl. Extracts were left 30 min on ice, passed 10 times through a 27-g needle, and centrifuged at full speed in a microfuge at 4°C for 10 min. One volume of protein sample buffer was added to the supernatant, and the sample was heated to 95°C for 3 min before analysis by SDS-PAGE. Immunoblotting was performed by electrophoretic transfer onto nitrocellulose membranes using a Semi-Phor blotting apparatus (Hoefer Scientific Instruments, San Francisco, CA). Proteins were visualized by Ponceau S staining, before blocking the membranes with blocking buffer (5% low-fat dried milk in 1× PBS + 0.1% Tween-20). All antibody incubations were carried out in blocking buffer, and bound IgGs were visualized using alkaline phosphatase–conjugated anti–rabbit IgG secondary antibodies (Promega Corp., Madison, WI). For in vitro phosphorylation of the COOH-terminal domain of C-Nap1, the myc:2-6 protein was in vitro translated from the pBSmyc:2-6 plasmid using a T3 polymerase with the TNT Coupled Reticulocyte Lysate System (Promega Corp.) in the presence of [^{35}S]methionine (Amersham Corp., Arlington Heights, IL). 10 μl of the in vitro translation reaction was then mixed with 50 μl of Nek2 kinase buffer (Fry and Nigg, 1997), in the presence or absence of [^{32}P-γ]ATP, and added to baculovirus-expressed wild-type or catalytically inactive Nek2 immunoprecipitates prepared as described in Fry and Nigg (1997). Samples were incubated at 30°C for 20 min, diluted 1:5 with NEB buffer (Fry and Nigg, 1997), and spun briefly in a microfuge, and the supernatant was recovered. For immunoprecipitation of myc-tagged proteins, samples were precleared for 1 h with protein G–Sepharose beads (Pharmacia Biotech) and then incubated for 1 h at 4°C with protein G–Sepharose beads previously coupled with anti-myc monoclonal antibody 9E10. Immunoprecipitates were finally washed four

times in NEB buffer, resuspended in 50 μl of protein sample buffer, and analyzed by SDS-PAGE.

cDNA Library Screening and Sequence Analysis

Overlapping cDNA clones spanning the entire coding sequence of C-Nap1 were isolated from a human placenta 5′-STRETCH PLUS cDNA library (CLONTECH Laboratories, Palo Alto, CA). DNA probes were labeled with ^{32}P using either the random-primed DNA labeling kit (Boehringer Mannheim, Mannheim, Germany) for larger DNA fragments or polynucleotide kinase (Biofinex, Praroman, Switzerland) for oligonucleotide probes. Positive phages were purified, lambda DNA was prepared from agarose plate lysates using the QIAGEN Lambda Kit, and inserts were excised and subcloned into the NotI site of a pBlueScript-KS vector. DNA sequencing in both directions was carried out using a 377 DNA Automated Sequencer (Perkin-Elmer Corp., Norwalk, CT).

Miscellaneous Techniques

Isolation of human centrosomes from the human T-lymphoblastic cell line KE37 was carried out as described previously (Moudjou and Bornens, 1994). Treatment of asynchronously growing U2OS cells with nocodazole or taxol was as described in Fry et al. (1998), while cold treatment was performed by placing the tissue culture dishes on ice for 30 min. RNA purification from mouse organs and RNase protection assays were performed as described in Tanaka et al. (1997). To prepare an antisense RNA probe for mouse C-Nap1, the transcript complementary to the intranuclear matrix protein (INMP) cDNA sequence (sequence data available from GenBank/EMBL/DDBJ under accession number U33198, nucleotides 1105–1733) was synthesized on an INMP cDNA fragment with T7 RNA polymerase (Promega Corp.) in the presence of 11.25 μM [α^{32}P]UTP (90 Ci/mmol, DuPont-NEN, Boston, MA). The template cDNA fragment was isolated by performing a reverse-transcriptase reaction on mouse testis RNA, followed by PCR amplification with specific primers corresponding to the 3′ and 5′ region of the published INMP sequence (Menz et al., 1996). For normalization, a transcript complementary to the mouse NF-Ya mRNA sequence was used (Tanaka et al., 1997).

For chromosomal mapping, two specific primers (AGCCACAGC-CAGGAGCACACAGAC and AGAGGCAGTACATGTCCCTCA-GCC) were used to amplify a 265-bp PCR fragment in the 3′ UTR of C-Nap1 using the Genbridge 4 Radiation Hybrid DNA panel (HGMP Resource Centre, UK). PCR products were analyzed by Southern blotting with a hybridization probe generated by PCR on the C-Nap1 cDNA, using the above oligonucleotides. The results were analyzed at http://www.genome.wi.mit.edu.

Results

Identification of a Centrosomal Protein through Two-Hybrid Interaction with Nek2

To identify cellular proteins that might interact with Nek2, a yeast two-hybrid screen was performed (Fields and Song, 1989; Durfee et al., 1993) using the full-length Nek2 as a bait. A human cDNA library was screened, and library clones able to activate both the auxotrophic selection marker His3 and the *lacZ* reporter gene specifically in the presence of the bait were selected. Among the clones showing a specific interaction with Nek2, three (designated 2-6, 2-27, and 2-31) were found to contain identical inserts of 1.7 kb, while a fourth (2-2) encoded a slightly longer version (1.9 kb) of the same cDNA. To determine which domains of Nek2 were required for the observed interactions, clones 2-6 and 2-2 were tested in the yeast two-hybrid assay against different Nek2 constructs (data not shown): both clones interacted strongly with full-length wild-type Nek2, a catalytically inactive mutant of Nek2 (Nek2-K37R; Fry et al., 1995), and the COOH-terminal noncatalytic domain of Nek2. There was also a significant interaction, albeit slightly less strong, with the NH2-termi-
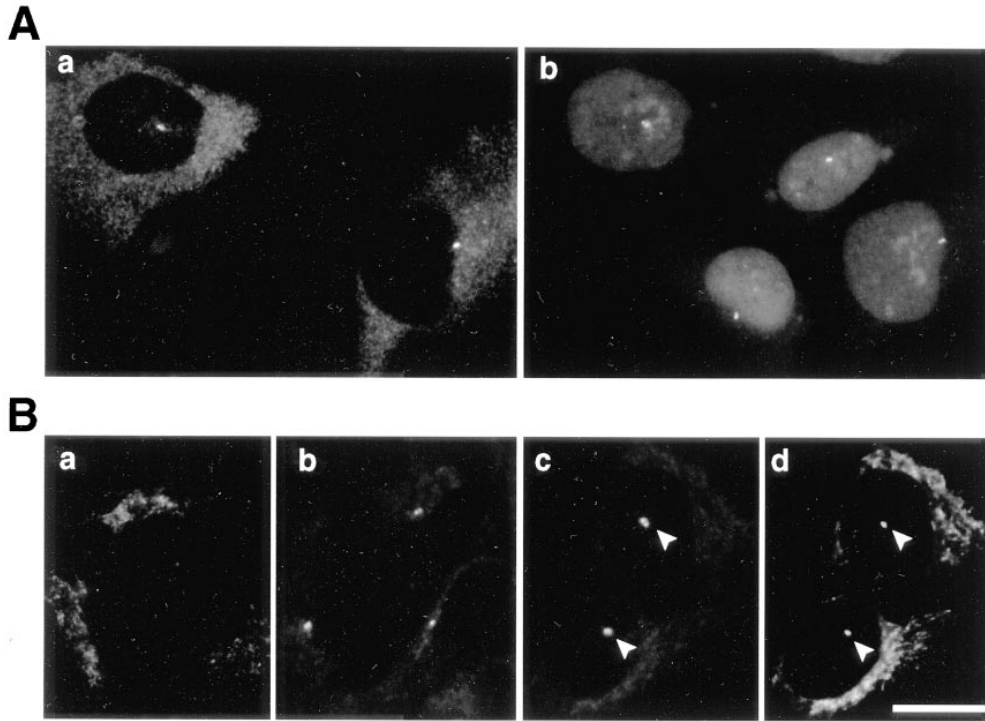
A

B

Figure 1. Localization of transfected and endogenous C-Nap1 to the centrosome. (*A*) U2OS osteosarcoma cells were transiently transfected with myc-epitope–tagged clone 2-6 and fixed with methanol after 24 h. Cells were double-stained with anti-myc (*a*) and anti–γ-tubulin (*b*) antibodies. In *b*, nuclei can be seen due to staining of the DNA with Hoechst dye 33258. (*B*) Asynchronous U2OS cells were fixed with methanol and stained with anti–C-Nap1 antibodies (*a*, preimmune R63; *b*, immune R63; *c*, immune R62). Cells stained for C-Nap1 (*c*) were also double-stained for the centrosomal component p150^{Glued} (*d*), demonstrating colocalization at the centrosome (*c* and *d*, *arrowheads*). Bar, 10 μm.

nal catalytic domain of Nek2, suggesting that these clones were binding both the catalytic and noncatalytic domains of Nek2. The COOH-terminal noncatalytic domain contains a leucine zipper motif that is implicated in Nek2 homodimerization (Fry, A.M., L. Arnaud, and E.A. Nigg, manuscript in preparation). Deletion of this leucine zipper did not reduce the strength of the association between Nek2 and clones 2-6 or 2-2, indicating that this motif was not by itself responsible for the observed interaction.

As a first approach to assess the significance of this interaction, the subcellular localization of the protein encoded by clone 2-6 was examined by transfecting a myc-tagged version of this cDNA into human tissue culture cells. Immunofluorescence microscopy revealed that ectopically expressed myc:2-6 protein localized primarily to the centrosome, as demonstrated by colocalization of anti-myc antibodies with antibodies for the centrosomal marker γ-tubulin (Fig. 1 *A*, *a* and *b*). In weakly expressing cells, the myc:2-6 protein appeared to be exclusively associated with the centrosome, but in cells expressing higher levels, myc:2-6 could also be seen in the cytoplasm (Fig. 1 *A*, *a*). To verify this localization, two rabbit antisera (R62 and R63) were raised against bacterially expressed, polyhistidine-tagged 2-6 protein. When used for immunofluorescent staining of human tissue culture cells, both antibodies produced highly specific staining of the centrosome (Fig. 1 *B*, *b* and *c*), whereas no such staining was observed with the corresponding preimmune sera (Fig. 1 *B*, *a* and data not shown). The identity of the stained organelles was confirmed by performing double labeling experiments, using R62 in combination with a monoclonal antibody against p150^{Glued}, a component of the dynactin complex that is known to concentrate at the centrosome (e.g., Blangy et al., 1997; Fig. 1 *B*, *d*). From these results, we conclude that the protein encoded by cDNA 2-6 is a novel component of

the centrosome. Hence, in the following we refer to this protein as C-Nap1.

C-Nap1 Is a High Molecular Mass Coiled-Coil Protein

To determine the size of the endogenous C-Nap1 protein, the anti–C-Nap1 antibodies (R62 and R63) were used for Western blotting. On total extracts of U2OS cells, both anti–C-Nap1 antibodies consistently identified a protein migrating at ∼250 kD that was not detected by the corresponding preimmune sera (Fig. 2, lanes *2* and *1*, respectively, and data not shown). When similar immunoblots were performed on total extracts prepared from the KE37 T-lymphoblastic cell line, both anti–C-Nap1 antibodies again recognized a protein migrating at 250 kD (Fig. 2, lane *3* and data not shown), and importantly, this protein was substantially enriched in centrosome preparations isolated from these cells (Fig. 2, lane *4*). Indeed, the level of enrichment of C-Nap1 in purified centrosomes was very similar to that observed for Nek2, previously determined to be in the order of 100-fold (Fig. 2, lanes *5* and *6*; and see Fry et al., 1998). Extrapolating from Nek2, this result also implies that the existence of a noncentrosomal pool of C-Nap1 is to be expected. Interestingly, both C-Nap1 antibodies also recognized a band at ∼190 kD in KE37 total cell extracts and centrosomal preparations (Fig. 2, lanes *3* and *4*). As this band showed a similar degree of enrichment in centrosome preparations as the full-length C-Nap1 protein, we believe that it may be structurally related (e.g., either represent a breakdown product of C-Nap1 or an alternatively spliced form; see legend to Fig. 3).

The above data strongly suggested that the C-Nap1 protein isolated originally by two-hybrid interaction with Nek2 represents a COOH-terminal fragment of a much larger protein. To obtain the full-length sequence, we
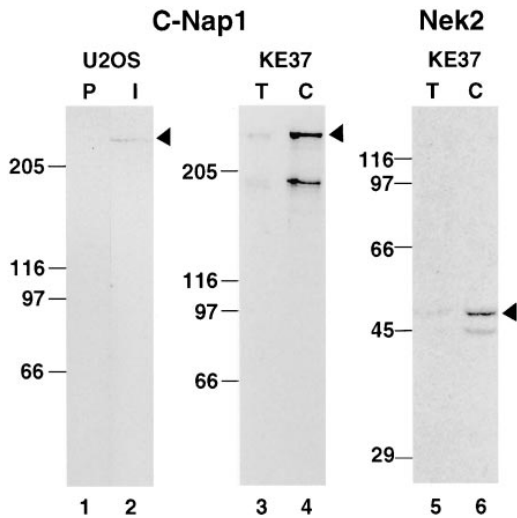
Figure 2. Anti–C-Nap1 antibodies recognize a high molecular mass protein in both whole cell extracts and isolated centrosomes. Cell extracts were prepared from exponentially growing U2OS cells (lanes *1* and *2*), separated on a 7.5% SDS–polyacrylamide gel, and probed by immunoblotting with anti–C-Nap1 antibodies (lane *1*, R63 preimmune; lane *2*, R63 immune). Alternatively, immunoblots were performed on total KE37 cell extracts (*T*, lanes *3* and *5*) and isolated KE37 centrosome preparations (*C*, lanes *4* and *6*), using antibodies against C-Nap1 (R63, lanes *3* and *4*; 7.5% gel) and, for comparison, Nek2 (R40, lanes *5* and *6*; 12% gel). Approximately 20 times more protein was loaded in the total extract than in the centrosome fraction, as determined by a comparison of the two samples on a silver-stained gel. The positions of molecular mass markers (kD) are indicated on the left of each gel, and arrowheads mark the positions of the relevant proteins on the right.

screened a human placenta cDNA library with the available C-Nap1 probe, and after repeated rounds of screening, isolated several overlapping cDNAs spanning a total of 8,347 nucleotides (Fig. 3 *A*). Conceptual translation of these cDNAs revealed the presence of a continuous open reading frame coding for a protein of 2,442 amino acids, with a calculated molecular mass of 281 kD (Fig. 3 *B*). Although we have been unable to determine the size of the C-Nap1 mRNA by Northern blot analysis, presumably because of the low abundance of this transcript (see below), we are confident that the isolated cDNAs encompass the complete protein. In fact, the putative initiator methionine is preceded by several stop codons, and the 3′ ends of some cDNAs include a polyadenylation signal and a polyA tail. Taken together with the results of our immunochemical data, these cDNA sequence analyses indicate that C-Nap1 is a novel, high molecular mass component of the mammalian centrosome. The C-Nap1 gene was mapped by radiation hybrid mapping close to the centromeric region of human chromosome 20, between the framework markers WI-6874 and AFMA152YG1. This places C-Nap1 between the genetic markers D20S195 and D20S908 at approximately 20q11.2.

Examination of the predicted C-Nap1 protein sequence indicates that this protein is likely to form extended coiled-coil domains, with a possible kink or hinge region near the center (Fig. 3 *C*). Database searches revealed that

the COOH terminus of C-Nap1 is almost identical to a previously described mouse protein, termed INMP (see Discussion). Furthermore, while this manuscript was in preparation, a human cDNA corresponding to the first 5 kb of the C-Nap1 sequence reported here was deposited in the Genbank database (under accession number AFO22655). In keeping with our results, this independently isolated cDNA was identified with the aid of human autoimmune sera reactive against centrosomal antigens (Mack et al., 1998). Beyond these matches, however, no obvious close relatives of C-Nap1 could be identified in any species, apart from weak similarities to many coiled-coil proteins.
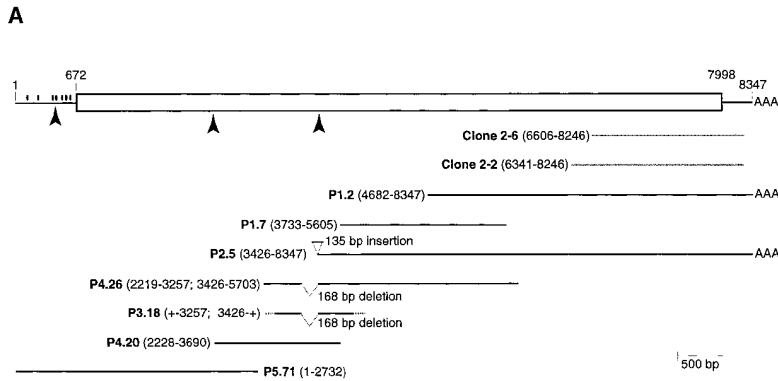
C-Nap1 Is a Low Abundance Ubiquitous Protein

Recent studies on the expression of Nek2 have shown that this kinase is highly abundant in testis, and detailed in situ hybridization analyses revealed a stage-specific expression pattern during spermatogenesis (Rhee and Wolgemuth, 1997; Tanaka et al., 1997). To investigate whether C-Nap1 might show a similar tissue-specific expression, we have isolated a cDNA coding for murine C-Nap1 and performed RNase protection experiments. As shown in Fig. 4, C-Nap1 was expressed ubiquitously and at comparable levels in all tissues analyzed, including testis. Thus, there is presently no evidence for a specialized function of C-Nap1 in meiotic processes. It is noteworthy, however, that the intensities of the signals observed with the C-Nap1 probe were similar to those obtained with a control probe for the ubiquitous transcription factor NF-Ya, labeled to a comparable specific activity (Fig. 4). As it has been calculated previously that there are only about 10 copies of the NF-Ya mRNA per cell (Schmidt and Schibler, 1995), our results would indicate that the level of C-Nap1 mRNA may be similarly low.

C-Nap1 Is a Centriole-associated Core Component of the Centrosome

To determine whether the centrosomal association of C-Nap1 was dependent upon the presence of microtubules, immunostaining on cells was performed under conditions that perturb the microtubule network. In cells incubated at 4°C for 30 min or treated with nocodazole for 4 h, interphase microtubules were completely depolymerized (Fig. 5, *b* and *c*). Yet, in comparison to untreated cells (Fig. 5, *a* and *e*), there was no observable decrease in the concentration of C-Nap1 at the centrosome after cold or nocodazole treatment (Fig. 5, *f* and *g*). In cells incubated with taxol, on the other hand, the microtubules appeared as dense bundles, which in many interphase cells were detached from the centrosome (Fig. 5 *d*). In such cells, C-Nap1 was clearly still associated with the centrosome and not with the microtubule bundles (Fig. 5 *h*). Thus, C-Nap1, like Nek2, associates with centrosomes independently of microtubules, and by this criterion, should be considered as a bona fide component of the core centrosome (Oegema et al., 1995).

To examine the localization of C-Nap1 at the ultrastructural level, immunoelectron microscopy (IEM) was performed, initially using anti–C-Nap1 antibodies on isolated centrosomes. After negative staining IEM, gold particles were specifically found at one end of the centriole (Fig. 6
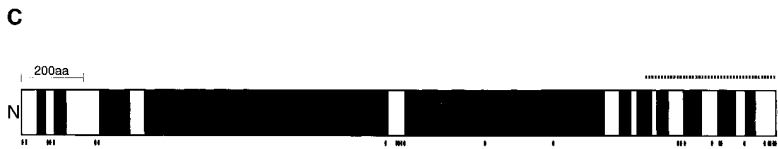
A

672 ... 7998 8347

Clone 2-6 (6606-8246)
Clone 2-2 (6341-8246)
P1.2 (4682-8347) —AAA
P1.7 (3733-5605)
P2.5 (3426-8347) ¬135 bp insertion —AAA
P4.26 (2219-3257; 3426-5703) — 168 bp deletion
P3.18 (+-3257; 3426-+) — 168 bp deletion
P4.20 (2228-3690)
P5.71 (1-2732)

500 bp

B

```
   1  METRSPGLNN  MKPQSLQLVL  BEQVLALQQQ  MAENQAASWR  KLKNSQEAQQ  RQATLVRKLQ  AKVLQYRSWC  QELEKRLEAT  GGPIPQRWEN
  91  VEEPNLDELL  VRLEEEQQRC  ESLAEVNTQL  RLHMEKADVV  NKALREDVEK  LTVDWSRARD  ELMRKESQWQ  MEQEFFKGYL  KGEHGRLLSL
 181  WREVVTFRRH  FLEMKSATDR  DLMELKAEHV  RLSGSLLTCC  LRLTVGAQSR  EPNGSGRMDG  REPAQLLLLL  AKTQELEKEA  HERSQELIQL
 271  KSQGDLEKAE  LQDRVTELSA  LLTQSQKQNE  DYEKMIKALR  ETVEILETNH  TELMEHEASL  SRNAQEEKLS  LQQVIKDITQ  VMVEEGDNIA
 361  QGSGHENSLE  LDSSIFSQFD  YQDADKALTL  VRSVLTRRRQ  AVQDLRQQLA  GCQEAVNLLQ  QQHDQWEEEG  KALRQRLQKL  TGERDTLAGQ
 451  TVDLQGEVDS  LSKERELLQK  AREELRQQLE  VLEQEAWRLR  RVNVELQLQG  DSAQGQKEDQ  QEELHLAVRE  RERLQRMLMG  LEAKQSESLS
 541  ELITLREALE  SSHLEGELLR  QEQTEVTAAL  ARAEQSIAEL  SSSENTLKTE  VADLRAAAVK  LSALNEALAL  DKVGLNQQLL  QLEEENQSVC
 631  SRMEAAEQAR  NALQVDLAEA  EKRRRALWEK  NTHLEAQLQK  AEEAGAELQA  DLRDIQEEKE  EIQKKLSESR  HQQEAATTQL  EQLHQEAKRQ
 721  EEVLARAVQE  KEALVREKAA  LEVRLQAVER  DRQDLAEQLQ  GLSSAKELLE  SSLFEAQQQN  SVIEVTKGQL  EVQIQTVTQA  KEVIQGEVRC
 811  LKLELDTERS  QAEQERDAAA  RQLAQAEQEG  KTALEQQKAA  HEKEVNQLRE  KWEKERSWHQ  QELAKALESL  EREKMELEMR  LKEQQTEMEA
 901  IQAQREEERT  QAESALCQMQ  LETEKERVSL  LETLLQTQKE  LADASQQLER  LRQDMKVQKL  KEQETTGILQ  TQLQEAQREL  KEAARQHRDD
 991  LAALQEESSS  LLQDKMDLQK  QVEDLKSQLV  AQDDSQRLVE  QEVQEKLRET  QEYNRIQKEL  EREKASLTLS  LMEKEQRLLV  LQEADSIRQQ
1081  RLSALRQDMQ  EAQGEQKELS  AQMELLRQRV  KEKEADFLAQ  RAQLLERLEA  SHITRQQLRA  SLWAQEAKAA  QLQLRLRSTR  SQLRALAAFQ
1171  QPGNQAQAQA  QLASLYSALQ  QALGSVCESR  PELSGGGDSA  PSVWGLEPDQ  NGARSLFKRG  PLLTALSAEA  VASALHKLHQ  DLWKTQQTRD
1261  VLRDQVQKLE  ERLTDTTEABK  SQVHTELQDL  QRQLSQNQEE  KSKWEGKQNS  LESELMELHE  TMASLQSRLR  RAELQRMEAQ  GERELLQAAK
1351  ENLTAQVEHL  QAAVVEARAQ  ASAAGILEED  LRTARSALKL  KNEEVESVLE  RAQALQEQGE  LKVAQGKALQ  ENLALLTQTL  AEREEEVETL
1441  RGQIQELEKQ  REMQKAALEL  LSLDLKKRNQ  EVDLQQPEQIQ  ELEKCRSVLE  HLPMAVQERE  QKLTVQREQI  RELEKDRETQ  RNVLEHQLLE
1531  LEKKDQMIES  QRGQVQDLKK  QLVTLECLAL  ELEENHHKME  CQQKLIKELE  GQRETQRVAL  THLTLDLEER  SQELQAQSSQ  IHDLESHSTV
1621  LARELQERDQ  EVKSQREQIE  ELQRQKEHLT  QDLERRDQEL  MLQKERIQVL  EDQRTRQTKI  LEEDLEQIKL  SLRERGRELT  TQRQLMQERA
1711  EEGKGPSKAQ  RGSLEHMKLI  LRDKEKEVEC  QQEHIHELQE  LKDQLEQQLQ  GLHRKVGETS  LLLSQREQEI  VVLQQQLQEA  REQGELKEQS
1801  LQSQLDEAQR  ALAQRDQELE  ALQQEQQQAQ  GQEERVKEKA  DALQGALEQA  HMTLKERHGE  LQDHKEQARR  LEEELAVEGR  RVQALEEVLG
1891  DLRAESREQE  KALLALQQQC  AQVEDLKSQLV  TRALQDSWLQ  AQAVLKERDQ  ELEALRAESQ  SSRHQEEAAR  ARAEALQEAL  GKAHAALQGK
1981  EQHLLBQABL  SRSLEASTAT  LQASLDACQA  HSRQLEEALR  IQEGEIQDQD  LRYQEDVQQL  QQALAQRDEE  LRHQQEREQL  LEKSLAQRVQ
2071  ENMIQKQNL  GQEREEBEIR  GLHQSVRELQ  LTLAQKEQEI  LELRETQQRN  NLEALPHSHK  TSPMEEQSLK  LDSLEPRLQR  ELERLQAALR
2161  QTEAREIEWR  EKAQDLALSL  AQTKASVSSL  QEVAMFLQAS  VLERDSEQQR  LQDELELTRR  ALEKERLHSP  GATSTAELGS  RGEQGVQLGE
2251  VSGVEAEPSP  DGMEKQSWRQ  RLEHLQQAVA  RLEIDRSRLQ  RHNVQLRSTL  EQVERERRKL  KREAMRAAQA  GSLEISKATA  SSPTQQDGRG
2341  QKNSDAKCVA  ELQKEVVLLQ  AQLTLERKQK  QDYITRSAQT  SRELAGLHHS  LSHSLLAVAQ  APEATVLEAE  TRRLDESLTQ  SLTSPGPVLL
2431  HPSPSTTQAA  SR•
```

C

200aa

N [C

Figure 3. Isolation of C-Nap1 cDNAs. (A) A schematic representation of the entire C-Nap1 cDNA, as deduced from the clones isolated from the yeast two-hybrid interaction screen (clones 2-6 and 2-2) and several placenta cDNA library screens (P). The nucleotides encoded by each cDNA are indicated in parentheses alongside the clone number. The exact length of clone P3.18 was not determined (*dotted lines*). In-frame stop codons in the 5′ untranslated region are indicated by dots, while the position of three putative introns, as based on the isolation of cDNAs presumably derived from partially processed transcripts, are denoted by arrowheads (at nt443, nt2242, and nt3425). Of particular interest, clone P2.5 has a 135-bp insertion at its 5′ end, which contains all the characteristic hallmarks of an intron; conversely, clones P3.18 and P4.26 both have a 168-bp in-frame deletion at the corresponding position. It seems most likely, therefore, that the 168-bp deletion in these two latter clones corresponds to an exon, and that these cDNAs represent an alternatively spliced, shorter form of C-Nap1. (B) The amino acid sequence of C-Nap1, as deduced from the cDNA nucleotide sequence. The 56–amino acid putative exon described as missing in clones P3.18 and P4.26 is underlined. (C) A schematic view of the C-Nap1 protein structure, showing the regions predicted to form coiled-coil structures (*black boxes*), as determined by analysis with the COILS program (version 2.1, window 28; Lupas, 1996). Dots underneath this schematic representation indicate the positions of proline residues, which usually disrupt coiled-coil secondary structures. The hatched bar above the COOH terminus denotes the region used to raise the anti–C-Nap1 antibodies, R62 and R63. These sequence data are available from the GenBank/EMBL/DDBJ database under accession number AF049105.

a). Whenever a pair of centrioles was visible, gold particles were consistently present at the proximal ends of each centriole (data not shown). Next, preembedding IEM was carried out, using anti–C-Nap1 antibodies on U2OS human osteosarcoma cells (Fig. 6, *b–g*). Again, the bulk of gold particles was tightly associated with the proximal ends of the centrioles. There were very few gold particles located elsewhere in the PCM, and little penetration into the lumen of the centriole barrel could be observed. In many sections, one centriole was more heavily labeled than the other; however, when serial sections through a pair of centrioles were compared, both centrioles showed proximal end labeling, suggesting that mother and daughter centrioles were labeled to a similar extent (Fig. 6, *b* and *c*). We have also performed preembedding IEM, using anti-Nek2 antibodies on U2OS cells. In this case, we observed a pattern of staining remarkably similar to that seen with anti–C-Nap1 antibodies, with a concentration of Nek2 also at the proximal ends of centrioles (Fig. 6, *h–k*). Hence, C-Nap1 and Nek2 demonstrate a striking colocalization within the substructure of the centrosome. Attesting to the specificity of these results, antibodies against γ-tubulin produced a much more diffuse labeling through-

out the PCM (data not shown), in agreement with previously published results (Fuller et al., 1995; Moudjou et al., 1996). Also, no centrosome-specific staining was observed when using the immunogold-labeled secondary antibodies alone (data not shown).

Loss of C-Nap1 Staining on Mitotic Spindle Poles

The intensity of centrosome staining by anti–C-Nap1 antibodies showed little if any variation during interphase stages of the cell cycle, and fairly uniform staining was also observed when anti–C-Nap1 antibodies were used to stain centrosomes isolated from exponentially growing KE37 cells (data not shown). In striking contrast, however, mitotic spindle poles were poorly labeled by anti–C-Nap1 antibodies, and in some mitotic cells staining of spindle poles was undetectable altogether (Fig. 7). Diminished C-Nap1 staining could be detected at the onset of prophase, concomitant with centrosome separation, increased microtubule-nucleating activity, and chromosome condensation (Fig. 7 *A*, *a–c*), and it persisted throughout the remainder of mitosis (e.g., anaphase cell in Fig. 7 *A*, *d* and *e*). The apparent loss of C-Nap1 from mitotic spindle poles is in
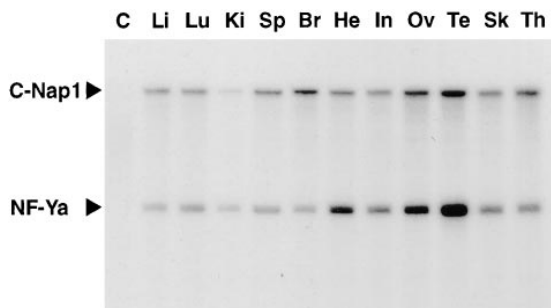
Figure 4. RNase protection analysis of C-Nap1 expression in mouse tissues. RNase protection experiments were performed on RNA corresponding to 10-μg DNA equivalents of each tissue (see Tanaka et al., 1997). Each RNA was supplemented to 100 μg with yeast RNA and hybridized with 10 fmol of both C-Nap1 and NF-Ya probes. The control (*C*) contained 100 μg yeast RNA and 10 fmol of each probe. All organs were isolated from 4-mo-old adult mice. *Li*, liver; *Lu*, lung; *Ki*, kidney; *Sp*, spleen; *Br*, brain; *He*, heart; *In*, intestine; *Ov*, ovary; *Te*, testis; *Sk*, skin; *Th*, thymus.

marked contrast to what is seen with many other centrosomal components, such as γ-tubulin, which show an increased accumulation at the spindle poles as a result of centrosome maturation in late G2 (Fig. 7 *B*, compare *a–d* with *e–h*). The most straightforward interpretation of these results is that the observed loss of C-Nap1 staining during mitosis reflects a significant reduction in the amount of C-Nap1 protein at mitotic spindle poles. However, we cannot rigorously exclude cell cycle–dependent epitope masking as an alternative explanation.

Phosphorylation of C-Nap1 by Nek2

The observed interaction between the COOH-terminal fragment of C-Nap1 and Nek2 raised the possibility that C-Nap1 might be a substrate of Nek2. To examine this

possibility, the myc-tagged C-Nap1 clone 2-6 (i.e., the COOH-terminal 53 kD of C-Nap1) was transcribed and translated in a rabbit reticulocyte lysate and incubated in the presence of recombinant Nek2 proteins immunoprecipitated from baculovirus-infected insect cells. In the presence of active Nek2, the myc:2-6 protein showed a drastic reduction in electrophoretic mobility (Fig. 8 *A*, lane *1*) and could be radiolabeled by incubation with [^{32}P-γ]ATP (Fig. 8 *A*, lane *3*), whereas neither of these results was observed in the presence of the catalytically inactive Nek2 mutant (Fig. 8 *A*, lanes *2* and *4*). Hence, Nek2 could readily phosphorylate the COOH-terminal fragment of C-Nap1 in vitro. To determine whether this was also the case in vivo, the C-Nap1 clone myc:2-6 was cotransfected with either active or inactive Nek2 into U2OS cells. 24 h after transfection, cells were lysed directly into hot sample buffer to prevent reactions proceeding during extraction, and the electrophoretic mobility of the myc:2-6 protein was examined by immunoblotting with anti-myc antibodies. Consistent with the data obtained in vitro, myc:2-6 showed a conspicuously reduced gel mobility when coexpressed with active Nek2 (Fig. 8 *B*, lane *3*), but not when expressed alone (Fig. 8 *B*, lane *2*) or in combination with the catalytically inactive Nek2 (Fig. 8 *B*, lane *4*). Thus, under the conditions used here, the COOH-terminal fragment of C-Nap1 behaves as a good substrate for Nek2 both in vitro and in living cells.

Discussion

Studies on the mammalian centrosome began more than a hundred years ago, yet many of its components still await identification, and the mechanisms regulating centrosome function during the cell cycle remain largely unknown. By combining genomic sequence information with analytical mass spectrometry, rapid progress is currently being made
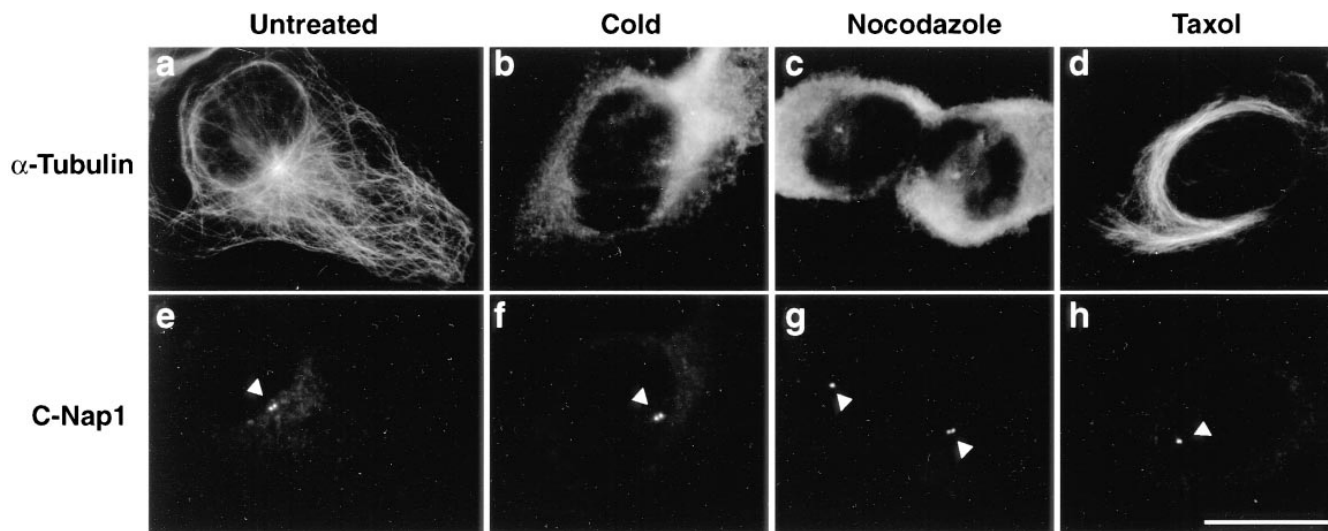

Figure 5. C-Nap1 association with the centrosome is independent of microtubules. Asynchronous U2OS cells, growing on coverslips, were either untreated (*a* and *e*), incubated for 30 min on ice (*b* and *f*), or treated for 4 h either with nocodazole (6 μg/ml; *c* and *g*) or taxol (5 μM; *d* and *h*). Cells were then fixed with methanol and double-stained for α-tubulin (*a–d*) and C-Nap1 (R63, *e–h*). C-Nap1 can still be seen associated with the centrosome (*arrowheads*, *e–h*) despite complete depolymerization of microtubules by cold treatment (*f*) or nocodazole (*g*), or taxol-induced detachment of microtubule bundles from the centrosome (*h*). Bar, 10 μm.
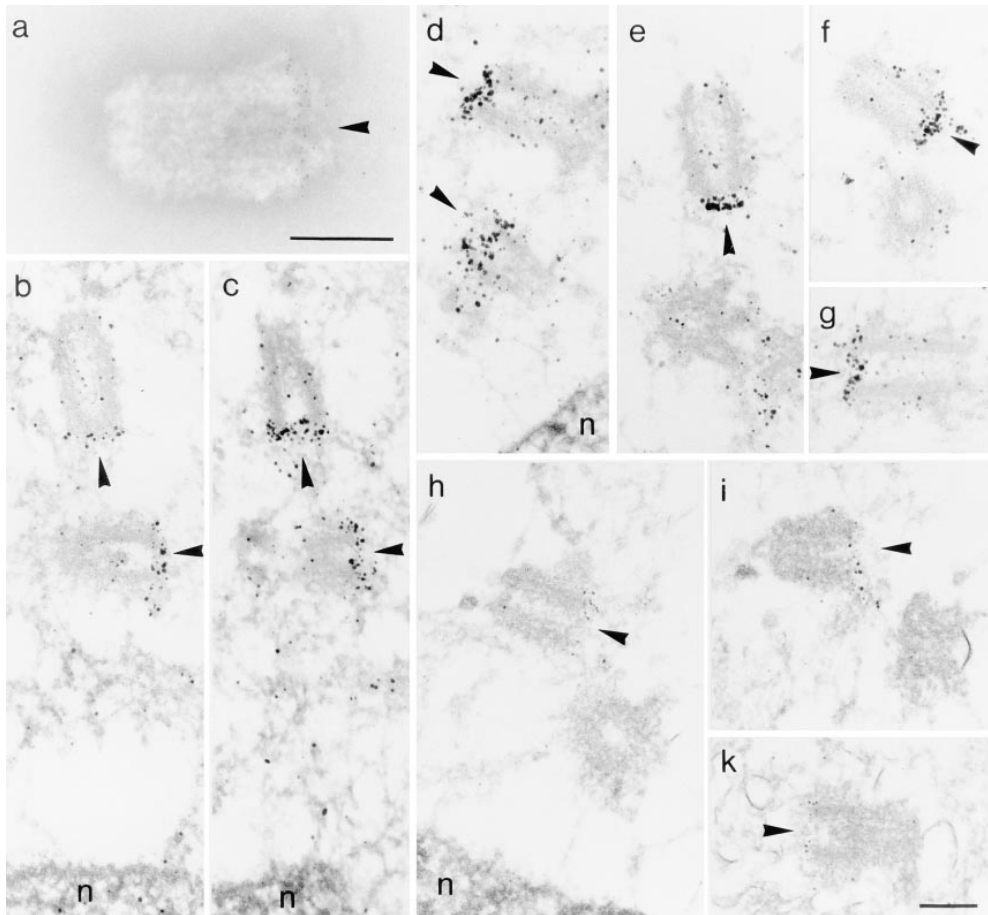
Figure 6. Ultrastructural analysis of C-Nap1 localization. Negative staining IEM was performed with affinity-purified C-Nap1 antibodies (R63) on isolated centrosomes prepared from KE37 cells (*a*). Preembedding immunoelectron microscopy was performed on U2OS cells (*b–k*) either with affinity-purified C-Nap1 antibodies (R63, *b–g*) or affinity-purified Nek2 antibodies (R40, *h–k*) together with silver-enhanced Nanogold. Arrowheads point to the labeled end of each centriole. *n*, nucleus. Bars: (*a*) 200 nm; (*b–k*) 500 nm.

on the identification of proteins present in spindle pole bodies (SPBs) purified from the yeast *Saccharomyces cerevisiae* (Rout and Kilmartin, 1990; Wigge et al., 1998). However, although many yeast SPB components may have been conserved during evolution, the substantial morphological differences between fungal SPBs and higher eukaryotic centrosomes suggest that this approach is unlikely to yield a complete inventory of the mammalian centrosome. Thus, complementary approaches for identifying novel centrosome components are needed. One straightforward strategy consists of the search for proteins that are able to interact with already known centrosomal proteins. Here, we have applied this strategy, using the centrosome-associated protein kinase Nek2 as a bait in a yeast two-hybrid screen. Through this approach, we have identified C-Nap1, a novel high molecular mass component of the centrosome. C-Nap1 not only colocalizes with Nek2 at the centrosome, but it also represents the first candidate physiological substrate of this cell cycle–regulated protein kinase.

Both immunocytological studies and biochemical analyses of purified centrosomes demonstrate that C-Nap1 is a bona fide component of the core centrosome. Furthermore, ultrastructural analyses using antibodies raised against the COOH terminus of C-Nap1 revealed a highly concentrated localization of the corresponding epitopes to the proximal ends of both mother and daughter centrioles. Although antigen accessibility is a general concern with preembedding IEM, this strikingly restricted localization is remarkable, as other centrosomal proteins show very different distributions within the centrosome: centrin was reported to be concentrated at the distal ends of centrioles, as well as within their lumen (Paoletti et al., 1996), whereas γ-tubulin has a broader distribution, localizing to the periphery of the PCM, to pericentriolar satellites and to the ends of centriolar and procentriolar microtubules (Fuller et al., 1995; Moudjou et al., 1996). Of those centrosomal proteins whose localization has been determined by electron microscopy, only a vertebrate Spc110p-related protein shows a localization somewhat similar to that described here for C-Nap1 (Tassin et al., 1997). However, while the Spc110p-related protein was reported to be associated preferentially with the mother centriole (Tassin et al., 1997), no biased distribution between mother and daughter centrioles could be detected in the case of C-Nap1, regardless of whether isolated centrosomes were analyzed or centrosomes in situ.

Cloning and sequencing of several overlapping cDNAs revealed that human C-Nap1 is a protein with a predicted molecular mass of 281 kD. The COOH terminus of C-Nap1 is very closely related to a previously described putative nuclear matrix protein, termed INMP, that was isolated by expression cloning using a monoclonal antibody raised to a nuclear matrix preparation (Menz et al., 1996). Based on cDNA sequencing, mouse INMP was reported to comprise 446 residues. However, our sequencing of C-Nap1 cDNAs isolated from both human placenta and mouse testis (Tanaka, K., T. Mayor, and E.A. Nigg, unpublished re-
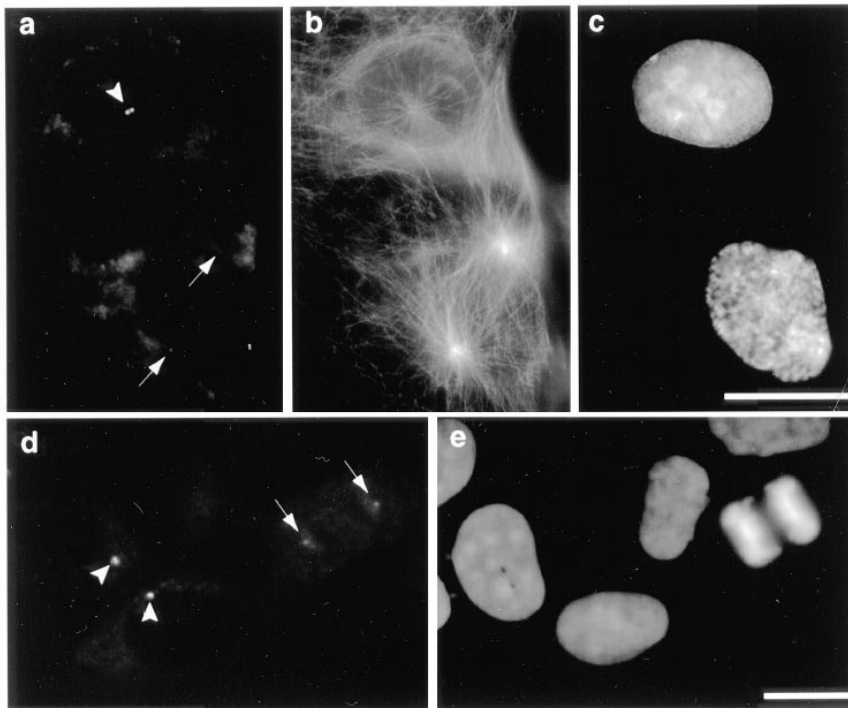
Figure 7. Loss of C-Nap1 immunoreactivity at mitotic spindle poles. (*A*) Exponentially growing U2OS cells were stained with anti–C-Nap1 antibody R63, and fields were photographed (*a* and *d*) in which the centrosomes in interphase cells (*arrowheads*) were in the same focal plane as the spindle poles in mitotic cells (*arrows*). In *a*, the lower cell is in prophase of mitosis, as indicated by the separation of microtubule-organizing centers (*b*, α-tubulin) and the condensation of chromatin (*c*, DNA). In *d*, the right-hand cell is in anaphase, as indicated by the separation of condensed chromosomes (*e*, DNA stain). (*B*) Direct comparison of C-Nap1 (*a–d*) and γ-tubulin (*e–h*) staining of interphase centrosomes (*a*, *b*, *e*, and *f*) and mitotic spindle poles (*c*, *d*, *g*, and *h*). Exposure times and image processing were identical between interphase and mitotic cells. Bars, 10 μm.
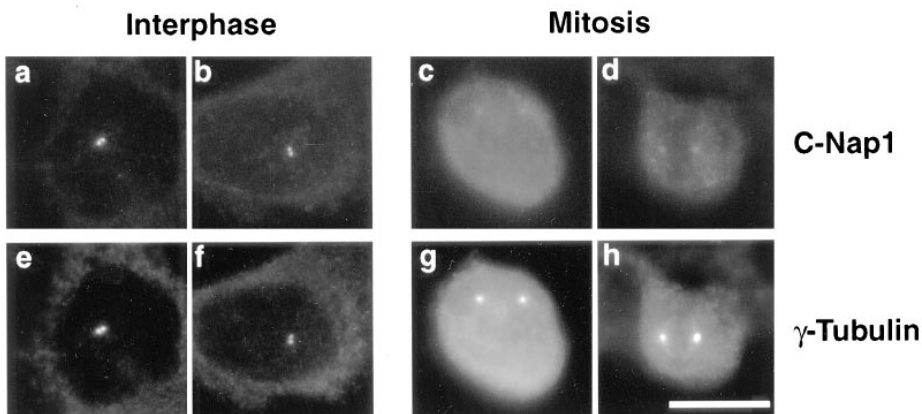
sults) libraries revealed that an open reading frame extends throughout the alleged 5′ untranslated region of INMP. Thus, we believe that INMP most likely represents a COOH-terminal fragment of a mouse C-Nap1 homologue. It would be premature to exclude the existence of C-Nap1–related proteins within the nucleus, but our localization studies provide no evidence for a nuclear localization of the C-Nap1 protein described here. Additional support that C-Nap1 is a bona fide centrosomal protein stems from the independent identification of the same protein in a study on the characterization of human autoimmune sera with centrosomal reactivity (Mack et al., 1998).

On the basis of primary structure analyses, C-Nap1 is predicted to consist almost entirely of coiled-coil domains (Lupas, 1996). Several other recently described centrosomal proteins also contain predicted coiled-coils (for review see Stearns and Winey, 1997), suggesting that protein–protein interactions based on such domains may be ideally suited for the maintenance of a dynamic centrosome structure. The only regions within C-Nap1 that contain clusters of helix-breaking proline residues are located towards the extreme NH$_2$ and COOH termini, and intriguingly, near the center of the protein. Thus, it is possible that C-Nap1 might contain a hinge or even fold back upon itself. Provided that recombinant C-Nap1 can be produced in a soluble form, it will be interesting to determine its shape. If this 281-kD coiled-coil protein were to form a straight rod, then its predicted length would be around 300 nm (comparable to the average intercentriolar distance; e.g., Chrétien et al., 1997). At present, we have no information about the oligomerization state of C-Nap1 or its ability to interact with other coiled-coil proteins. However, electron-dense filaments have been shown to extend between the proximal ends of the two centrioles (Bornens et al., 1987; Paintrand et al., 1992; and references therein), and it is attractive to speculate that C-Nap1 could be a component of a
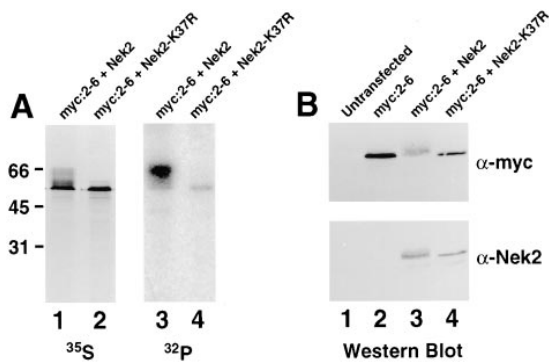
Figure 8. Phosphorylation of the COOH-terminal fragment of C-Nap1 by Nek2 in vitro and in vivo. (A) The C-Nap1 COOH-terminal construct myc:2-6 was in vitro translated in the presence of [^{35}S]methionine and then mixed with immunoprecipitates of recombinant wild-type Nek2 (lanes 1 and 3) or catalytically inactive Nek2 (lanes 2 and 4) for 20 min at 30°C in the absence (lanes 1 and 2) or presence (lanes 3 and 4) of [^{32}P]ATP. The Nek2 immunoprecipitates were then removed, and the myc:2-6 proteins were immunoprecipitated with anti-myc antibodies. Proteins were resolved on 12% SDS–polyacrylamide gels and subjected to autoradiography. To selectively enhance the signal due to ^{32}P (lanes 3 and 4), an additional piece of x-ray film was used to block the signal caused by ^{35}S; the faint band corresponding to the size of myc:2-6 in lane 4 is most likely due to weak penetration of the ^{35}S signal. Molecular mass markers (kD) are indicated on the left. (B) 10-cm dishes of exponentially growing U2OS cells were transiently transfected with no DNA (lane 1), 25 μg pCMV-myc:2-6 (lane 2), 12.5 μg pCMV-myc:2-6 + 12.5 μg pCMV-Nek2 (lane 3), or 12.5 μg pCMV-myc:2-6 + 12.5 μg pCMV-Nek2-K37R (lane 4). After 24 h, cell extracts were resolved on 12% SDS–polyacrylamide gels and immunoblotted with anti-myc antibodies (top) or anti-Nek2 antibodies (bottom). The C-Nap1 myc:2-6 protein exhibits a significant reduction in gel mobility specifically in the presence of active Nek2 both in vitro and in vivo.
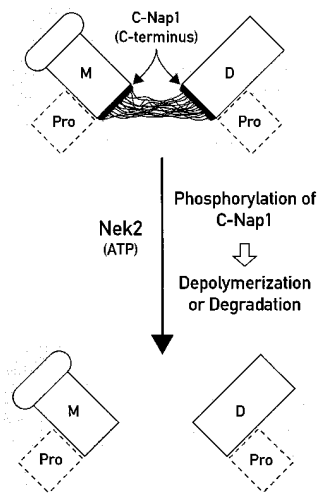

Figure 9. A possible role for C-Nap1 in centriole–centriole cohesion? This highly speculative model proposes that C-Nap1 may function as part of the intercentriolar link that connects the proximal ends of centrioles to each other during interphase. Anti–C-Nap1 antibodies stained the proximal ends of both centrioles (black bars), and since these antibodies were raised to the COOH terminus, it is attractive to postulate that C-Nap1 may form antiparallel or head-to-head oligomers connecting centrioles. To distinguish between these possibilities, it will be interesting to stain centrosomes with antibodies directed against other regions of the C-Nap1 protein. According to the model shown here, loss of centriole–centriole cohesion must occur at the onset of mitosis to allow the separation of duplicated centrosomes in preparation for spindle formation. By phosphorylating C-Nap1, Nek2 (or other kinases with related substrate specificity) may cause depolymerization or degradation of C-Nap1. This, in turn, would lead to the loss of the intercentriolar link and thereby permit centrosome splitting. Consistent with this model, endogenous Nek2 is active in G2 but not G1 cells (Fry et al., 1995), while overexpressed active Nek2 promotes premature centrosome splitting (Fry et al., 1998). The letters M and D denote the mother (depicted schematically with a distal appendage) and daughter centriole, respectively, while Pro refers to procentrioles. Finally, wavy lines highlight the proposed intercentriolar link, and the remainder of the PCM is indicated by gray shading.

structure connecting the proximal ends of centrioles to each other (Fig. 9).

In this context, it is intriguing that Nek2 is able to phosphorylate the COOH-terminal domain of C-Nap1 both in vitro and in vivo, suggesting that C-Nap1 may be a physiological substrate of Nek2. This invites speculations as to the mechanisms by which overexpression of Nek2 disrupts centrosome structure. In a previous study, we have shown that overexpression of Nek2 in cultured cells produces a striking splitting of centrosomes (Fry et al., 1998). Since this effect was strictly dependent on Nek2 activity, we have proposed that increased Nek2 activity may lead to the degradation or disassembly of a molecular "glue" that holds the two centrosomes in close apposition during most stages of the cell cycle. In the simplest interpretation of this model, the hypothetical glue would be composed of structural proteins, at least one of which would be a direct substrate of Nek2. Phosphorylation of this protein at the appropriate stage of the cell cycle could then either target it for degradation or cause it to dissociate from centrosomes, with both processes leading to a weakening of centriole–centriole cohesion. As C-Nap1 most likely fulfills a structural role and clearly can be phosphorylated by Nek2, it would seem to qualify as a candidate component of this hypothetical centrosomal glue (Fig. 9). We have ob-

served that C-Nap1 immunoreactivity is severely diminished at the spindle poles of mitotic cells, consistent with the notion that the association of C-Nap1 with the centrosome may be cell cycle regulated. However, as yet we have no information on either the timing or the molecular consequences of C-Nap1 phosphorylation by Nek2, and the model shown in Fig. 9 should therefore be considered as a working hypothesis. Testing of this model will require a detailed analysis of C-Nap1 phosphorylation during the cell cycle, and the mapping of Nek2-dependent phosphorylation sites. Such information may then set the stage for directly testing the consequences of overexpressing wild-type and phosphorylation-site mutant versions of C-Nap1 in living cells.

References

Blangy, A., L. Arnaud, and E.A. Nigg. 1997. Phosphorylation by p34[cdc2] protein kinase regulates binding of the kinesin-related motor HsEg5 to the dynactin subunit p150[Glued]. *J. Biol. Chem.* 272:19418–19424.

Blangy, A., H.A. Lane, P. d'Heren, M. Harper, M. Kress, and E.A. Nigg. 1995. Phosphorylation by p34[cdc2] regulates spindle association of human Eg5, a kinesin-related motor essential for bipolar spindle formation in vivo. *Cell.* 83:1159–1169.

Bornens, M., M. Paintrand, J. Berges, M.-C. Marty, and E. Karsenti. 1987. Structural and chemical characterization of isolated centrosomes. *Cell Motil. Cytoskel.* 8:238–249.

Brinkley, B.R. 1985. Microtubule organizing centers. *Annu. Rev. Cell Biol.* 1:145–172.

Buendia, B., G. Draetta, and E. Karsenti. 1992. Regulation of the microtubule nucleating activity of centrosomes in *Xenopus* egg extracts: role of cyclin A–associated protein kinase. *J. Cell Biol.* 116:1431–1442.

Centonze, V.E., and G.G. Borisy. 1990. Nucleation of microtubules from mitotic centrosomes is modulated by a phosphorylated epitope. *J. Cell Sci.* 95:405–411.

Chrétien, D., B. Buendia, S.D. Fuller, and E. Karsenti. 1997. Reconstruction of the centrosome cycle from cryoelectron micrographs. *J. Struct. Biol.* 120:117–133.

Dictenberg, J.B., W. Zimmerman, C.A. Sparks, A. Young, C. Vidair, Y. Zheng, W. Carrington, F.S. Fay, and S.J. Doxsey. 1998. Pericentrin and γ-tubulin form a protein complex and are organized into a novel lattice at the centrosome. *J. Cell Biol.* 141:163–174.

Doxsey, S., P. Stein, L. Evans, P.D. Calarco, and M. Kirschner. 1994. Pericentrin, a highly conserved centrosome protein involved in microtubule organization. *Cell.* 76:639–650.

Durfee, T., K. Becherer, P.-L. Chen, S.-H. Yeh, Y. Yang, A.E. Kilburn, W.-H. Lee, and S.J. Elledge. 1993. The retinoblastoma protein associates with the protein phosphatase type 1 catalytic subunit. *Genes Dev.* 7:555–569.

Fields, S., and O. Song. 1989. A novel genetic system to detect protein-protein interactions. *Nature.* 340:245–246.

Fry, A.M., and E.A. Nigg. 1995. Cell cycle. The NIMA kinase joins forces with Cdc2. *Curr. Biol.* 5:1122–1125.

Fry, A.M., and E.A. Nigg. 1997. Characterization of mammalian NIMA-related kinases. *Methods Enzymol.* 283:270–282.

Fry, A.M., S.J. Schultz, J. Bartek, and E.A. Nigg. 1995. Substrate specificity and cell cycle regulation of the Nek2 protein kinase, a potential human homolog of the mitotic regulator NIMA of *Aspergillus nidulans. J. Biol. Chem.* 2705:12899–12905.

Fry, A.M., P. Meraldi, and E.A. Nigg. 1998. A centrosomal function for the human Nek2 protein kinase, a member of the NIMA-family of cell cycle regulators. *EMBO (Eur. Mol. Biol. Organ.) J.* 17:470–481.

Fuller, S.D., B.E. Gowen, S. Reinsch, A. Sawyer, B. Buendia, R. Wepf, and E. Karsenti. 1995. The core of the mammalian centriole contains γ-tubulin. *Curr. Biol.* 5:1384–1393.

Geissler, S., G. Pereira, A. Spang, M. Knop, S. Soues, J. Kilmartin, and E. Schiebel. 1996. The spindle pole body component Spc98p interacts with the γ-tubulin-like Tub4p of *Saccharomyces cerevisiae* at the sites of microtubule attachment. *EMBO (Eur. Mol. Biol. Organ.) J.* 15:3899–3911.

Gould, R.R., and G.G. Borisy. 1977. The pericentriolar material in Chinese hamster ovary cells nucleates microtubule formation. *J. Cell Biol.* 73:601–615.

Gu, J., C.G. Stephenson, and M.J. Iadarola. 1994. Affinity purification of antibodies using a 6xHis-tagged antigen immobilized on Ni-NTA. *Biotechniques.* 17:257–262.

Harlow, E., and D. Lane. 1988. Antibodies: A Laboratory Manual. Cold Spring Harbor Laboratory Press, Cold Spring Harbor, NY. 313–315.

Harper, J.W., G.R. Adami, N. Wei, K. Keyomarsi, and S.J. Elledge. 1993. The p21 Cdk-interacting protein Cip1 is a potent inhibitor of G1 cyclin-dependent kinases. *Cell.* 75:805–816.

Kalt, A., and M. Schliwa. 1993. Molecular components of the centrosome. *Trends Cell Biol.* 3:118–128.

Karsenti, E. 1991. Mitotic spindle morphogenesis in animal cells. *Semin. Cell Biol.* 2:251–260.

Kellogg, D.R., M. Moritz, and B.M. Alberts. 1994. The centrosome and cellular organization. *Annu. Rev. Biochem.* 63:639–674.

Kimble, M., and R. Kuriyama. 1992. Functional components of microtubule-organizing centers. *Int. Rev. Cytol.* 136:1–50.

Knop, M., G. Pereira, S. Geissler, K. Grein, and E. Schiebel. 1997. The spindle pole body component Spc97p interacts with the γ-tubulin of *Saccharomyces cerevisiae* and functions in microtubule organization and spindle pole body duplication. *EMBO (Eur. Mol. Biol. Organ.) J.* 16:1550–1564.

Kochanski, R.S., and G.G. Borisy. 1990. Mode of centriole duplication and distribution. *J. Cell Biol.* 110:1599–1605.

Krek, W., and E.A. Nigg. 1991. Mutations of p34cdc2 phosphorylation sites induce premature mitotic events in HeLa cells: evidence for a double block to p34cdc2 kinase activation in vertebrates. *EMBO (Eur. Mol. Biol. Organ.) J.* 10:3331–3341.

Kuriyama, R., and G.G. Borisy. 1981*a*. Centriole cycle in Chinese hamster ovary cells as determined by whole-mount electron microscopy. *J. Cell Biol.* 91:814–821.

Kuriyama, R., and G.G. Borisy. 1981*b*. Microtubule-nucleating activity of cen-

trosomes in Chinese hamster ovary cells is independent of the centriole cycle but coupled to the mitotic cycle. *J. Cell Biol.* 91:822–826.

Lane, H.A., and E.A. Nigg. 1996. Antibody microinjection reveals an essential role for human polo-like kinase 1 (Plk1) in the functional maturation of mitotic centrosomes. *J. Cell Biol.* 135:1701–1713.

Lange, B.M.H., and K. Gull. 1995. A molecular marker for centriole maturation in the mammalian cycle. *J. Cell Biol.* 130:919–927.

Lange, B.M.H., and K. Gull. 1996. Structure and function of the centriole in animal cells: progress and questions. *Trends Cell Biol.* 6:348–352.

Lu, K.P., and T. Hunter. 1995*a*. The NIMA kinase: a mitotic regulator in *Aspergillus nidulans* and vertebrate cells. *In* Progress in Cell Cycle Research. Vol. 1. L. Meijer, S. Guidet, and H.Y.L. Tung, editors. Plenum Press, NY. 187–205.

Lu, K.P., and T. Hunter. 1995*b*. Evidence for a NIMA-like mitotic pathway in vertebrate cells. *Cell.* 81:413–424.

Lupas, A. 1996. Prediction and analysis of coiled-coil structures. *Methods Enzymol.* 266:513–525.

Mack, G.J., J. Rees, O. Sandblom, R. Balczon, M.J. Fritzler, and J.B. Rattner. 1998. Autoantibodies to a group of centrosomal proteins in human autoimmune sera reactive with the centrosome. *Arthritis Rheum.* 41:551–558.

Mazia, D. 1987. The chromosome cycle and the centrosome cycle in the mitotic cycle. *Int. Rev. Cytol.* 100:49–92.

McGill, M., and B.R. Brinkley. 1975. Human chromosomes and centrioles act as nucleating sites for the in vitro assembly of microtubules from bovine brain tubulin. *J. Cell Biol.* 67:189–199.

Menz, K., N. Radomski, and E. Jost. 1996. INMP, a novel intranuclear matrix protein related to the family of intermediate filament-like proteins: molecular cloning and sequence analysis. *Biochim. Biophys. Acta.* 1309:14–20.

Moritz, M., M.B. Braunfeld, J.W. Sedat, B. Alberts, and D.A. Agard. 1995. Microtubule nucleation by γ-tubulin-containing rings in the centrosome. *Nature.* 378:638–640.

Moudjou, M., and M. Bornens. 1994. Isolation of centrosomes from cultured animal cells. *In* Cell Biology: A Laboratory Handbook. Vol. 1. J.E. Celis, editor. Academic Press, Inc., London. 595–604.

Moudjou, M., N. Bordes, M. Paintrand, and M. Bornen. 1996. γ-Tubulin in mammalian cells: the centrosomal and the cytosolic forms. *J. Cell Sci.* 109:875–887.

O'Connell, M.J., C. Norbury, and P. Nurse. 1994. Premature chromatin condensation upon accumulation of NIMA. *EMBO (Eur. Mol. Biol. Organ.) J.* 13:4926–4937.

Oegema, K., W.G.F. Whitfield, and B. Alberts. 1995. The cell cycle–dependent localization of the CP190 centrosomal protein is determined by the coordinate action of two separable domains. *J. Cell Biol.* 131:1261–1273.

Osmani, A.H., S.L. McGuire, and S.A. Osmani. 1991. Parallel activation of the NIMA and p34cdc2 cell cycle-regulated protein kinases is required to initiate mitosis in *A. nidulans. Cell.* 67:283–291.

Osmani, S.A., and X.S. Ye. 1996. Cell cycle regulation in Aspergillus by two protein kinases. *Biochem. J.* 317:633–641.

Paintrand, M., M. Moudjou, H. Delacroix, and M. Bornens. 1992. Centrosome organization and centriole architecture: their sensitivity to divalent cations. *J. Struct. Biol.* 108:107–128.

Paoletti, A., M. Moudjou, M. Paintrand, J.L. Salisbury, and M. Bornens. 1996. Most of centrin in animal cells is not centrosome-associated and centrosomal centrin is confined to the distal lumen of centrioles. *J. Cell Sci.* 109:3089–3102.

Pu, R.T., G. Xu, L. Wu, J. Vierula, K. O'Donnell, X.S. Ye, and S.A. Osmani. 1995. Isolation of a functional homolog of the cell cycle-specific NIMA protein kinase of *Aspergillus nidulans* and functional analysis of conserved residues. *J. Biol. Chem.* 270:18110–18116.

Rhee, K., and D.J. Wolgemuth. 1997. The NIMA-related kinase 2, Nek2, is expressed in specific stages of the meiotic cell cycle and associates with meiotic chromosomes. *Development (Camb.).* 124:2167–2177.

Rieder, C.L., and G.G. Borisy. 1982. The centrosome cycle in PtK₂ cells: asymmetric distribution and structural changes in the pericentriolar material. *Biol. Cell.* 44:117–132.

Rout, M.P., and J.V. Kilmartin. 1990. Components of the yeast spindle pole body. *J. Cell Biol.* 111:1913–1927.

Sawin, K.E., and T.J. Mitchison. 1995. Mutations in the kinesin-like protein Eg5 disrupting localization to the mitotic spindle. *Proc. Natl. Acad. Sci. USA.* 92:4289–4293.

Schmidt, E.E., and U. Schibler. 1995. Cell size regulation, a mechanism that controls cellular RNA accumulation: consequences on regulation of the ubiquitous transcription factors Oct1 and NF-Y, and the liver-enriched transcription factor DBP. *J. Cell Biol.* 128:467–483.

Schmidt-Zachmann, M.S., and E.A. Nigg. 1993. Protein localization to the nucleolus: a search for targetting domains in nucleolin. *J. Cell Sci.* 105:799–806.

Schultz, S.J., A.M. Fry, C. Sütterlin, T. Ried, and E.A. Nigg. 1994. Cell cycle-dependent expression of Nek2, a novel human protein kinase related to the NIMA mitotic regulator of *Aspergillus nidulans. Cell Growth Diff.* 5:625–635.

Slot, J., and H.J. Geuze. 1985. A new method of preparing gold probes for multiple-labeling cytochemistry. *Eur. J. Cell Biol.* 38:87–93.

Snyder, J.A., and J.R. McIntosh. 1975. Initiation and growth of microtubules from mitotic centers in lysed mammalian cells. *J. Cell Biol.* 67:744–760.

Stearns, T., and M. Winey. 1997. The cell center at 100. *Cell.* 91:303–309.

Stierhof, Y.-D., B.M. Humbel, and H. Schwarz. 1991. Suitability of different silver enhancement methods applied to 1 nm colloidal gold particles: an immunoelectron microscopic study. *J. Electron Microsc. Tech.* 17:336–343.

Tanaka, K., M. Parvinen, and E.A. Nigg. 1997. The *in vivo* expression pattern

of mouse Nek2, a NIMA-related kinase, indicates a role in both mitosis and meiosis. *Exp. Cell Res.* 237:264–274.

Tassin, A.M., C. Celati, M. Paintrand, and M. Bornens. 1997. Identification of an Spc110p-related protein in vertebrates. *J. Cell Sci.* 110:2533–2545.

Tournier, F., and M. Bornens. 1994. Cell cycle regulation of centrosome function. *In* Microtubules. Wiley-Liss, Inc., New York. 303–324.

Vandré, D.D., F.M. Davis, P.N. Rao, and G.G. Borisy. 1984. Phosphoproteins are components of mitotic microtubule organising centers. *Proc. Natl. Acad. Sci. USA.* 81:4439–4443.

Vandré, D.D., F.M. Davis, P.N. Rao, and G.G. Borisy. 1986. Distribution of cytoskeletal proteins sharing a conserved phosphorylated epitope. *Eur. J. Cell Biol.* 41:72–81.

Verde, F., J.-C. Labbé, M. Dorée, and E. Karsenti. 1990. Regulation of microtubule dynamics by cdc2 protein kinase in cell-free extracts of *Xenopus* eggs.

Nature. 343:233–238.

Verde, F., M. Dogterom, E. Stelzer, E. Karsenti, and S. Leibler. 1992. Control of microtubule dynamics and length by cyclin A– and B–dependent kinases in *Xenopus* egg extracts. *J. Cell Biol.* 118:1097–1108.

Vorobjev, I.A., and Y.S. Chentsov. 1982. Centrioles in the cell cycle. I. Epithelial cells. *J. Cell Biol.* 98:938–949.

Vorobjev, I.A., and E.S. Nadehzdina. 1987. The centrosome and its role in the organization of microtubules. *Int. Rev. Cytol.* 106:227–284.

Wigge, P.A., O.N. Jensen, S. Holmes, S. Souès, M. Mann, and J.V. Kilmartin. 1998. Analysis of the *Saccharomyces* spindle pole by matrix-assisted laser desorption/ionization (MALDI) mass spectrometry. *J. Cell Biol.* 141:967–977.

Zheng, Y., M.L. Wong, B. Alberts, and T. Mitchison. 1995. Nucleation of microtubule assembly by a γ-tubulin-containing ring complex. *Nature.* 378:578–583.